Use of Penalty Formulations in Dynamic Simulation and Analysis of Redundantly Constrained Multibody Systems

Francisco González, József Kövecses

This is a post-peer-review, pre-copyedit version of an article published in Multibody System Dynamics. The final authenticated version is available online at: https://doi.org/10.1007/s11044-012-9322-y.

Multibody System Dynamics manuscript No.
(will be inserted by the editor)

Use of Penalty Formulations in Dynamic Simulation and Analysis of Redundantly Constrained Multibody Systems

Francisco González · József Kövecses

Received: date / Accepted: date

Abstract The determination of particular reaction forces in the analysis of redundantly constrained multibody systems requires the consideration of the stiffness distribution in the system. This can be achieved by modelling the components of the mechanical system as flexible bodies. An alternative to this, which we will discuss in this paper, is the use of penalty factors already present in augmented Lagrangian formulations as a way of introducing the structural properties of the physical system into the model. Natural coordinates and the kinematic constraints required to ensure rigid body behaviour are particularly convenient for this. In this paper, scaled penalty factors in an index-3 augmented Lagrangian formulation are employed, together with modelling in natural coordinates, to represent the structural properties of redundantly constrained multibody systems. Forward dynamic simulations for two examples are used to illustrate the material. Results showed that scaled penalty factors can be used as a simple and efficient way to accurately determine the constraint forces in the presence of redundant constraints.

Keywords Redundant constraints · Augmented Lagrangian formulation · Reaction forces · Penalty factors · Natural coordinates

1 Introduction

The field of Mechanics generally deals with models that rely on certain assumptions. These models give approximations for various behaviours of mechanical systems. They never fully represent physical reality, but address some important characteristics that give useful information about the real system. A key issue in the applications of Mechanics is how the models can relate to and characterize real physical systems. For example, point mass, rigid and flexible body models are commonly employed to represent elements of mechanical systems. The connections among these elements can generally be represented by giving force

F. González · J. Kövecses
Department of Mechanical Engineering and Centre for Intelligent Machines, McGill University
817 Sherbrooke St. West, Montréal, Québec, H3A 2K6, Canada
Tel.: +1-514-398-6302
E-mail: franglez@cim.mcgill.ca
E-mail: jozsef.kovecses@mcgill.ca

or motion specifications. Motion specifications are represented by kinematic constraints. Both body models and constraints are representational tools only to develop system models that are descriptive for a physical system. The use of these tools can lead to system models that contain constraints that are not independent of each other, i.e., redundantly constrained systems. These can often be necessary to keep models simple, e.g. the use of rigid body models, but also representative. For example, enhancing the structural integrity of a mechanical system can lead to redundantly constrained models. An example for this can be the most typical, type-A planetary gear train [32], where the use of one planet gear would be completely enough from the kinematics point of view. Despite this, often, three planet gears are employed to improve the load bearing capacity of the system.

The issue of dealing with redundant constraints comes into play also frequently in the development of multibody system models using generic algorithms. For example, if we build the model of a "planar" four-bar linkage using a general three-dimensional rigid body models based algorithm, then we arrive at a redundantly constrained model where some of the constraints are redundant from the kinematics point of view, as the particular motion to be enforced by them is already restrained by other constraints.

Let us consider that the configuration of a mechanical system is fully defined by a set of n generalized coordinates $\mathbf{q}$. The presence of redundant constraints adds additional complexity to the analysis of the equations of motion, usually given as

$$\mathbf{M}\ddot{\mathbf{q}} + \mathbf{c} = \mathbf{f}_a + \mathbf{f}_c \tag{1}$$

where $\mathbf{M}$ stands for the mass matrix of the system, $\mathbf{f}_c$ is the array of generalized constraint forces and $\mathbf{f}_a$ and $\mathbf{c}$ stand for the vectors of generalized applied forces and Coriolis and centrifugal effects, respectively. For the purposes of this work, we will consider that the motion of the system is restricted by a set of m holonomic constraint equations

$$\mathbf{\Phi}\left(\mathbf{q}, t\right) = \mathbf{0} \tag{2}$$

which, at velocity and acceleration levels, can be described as

$$\mathbf{A}\dot{\mathbf{q}} + \mathbf{b} = \mathbf{0} \tag{3}$$

and

$$\mathbf{A}\ddot{\mathbf{q}} + \dot{\mathbf{A}}\dot{\mathbf{q}} + \dot{\mathbf{b}} = \mathbf{0} \tag{4}$$

with the Jacobian matrix $\mathbf{A} = \partial\mathbf{\Phi}/\partial\mathbf{q}$ and $\mathbf{b} = \partial\mathbf{\Phi}/\partial t$. The dynamic equations of the system (1) can be expressed together with the constraints at acceleration level (4) as

$$\begin{bmatrix} \mathbf{M} & -\mathbf{A}^{\mathrm{T}} \\ -\mathbf{A} & \mathbf{0} \end{bmatrix} \begin{bmatrix} \ddot{\mathbf{q}} \\ \boldsymbol{\lambda} \end{bmatrix} = \begin{bmatrix} \mathbf{f}_a - \mathbf{c} \\ \dot{\mathbf{A}}\dot{\mathbf{q}} + \dot{\mathbf{b}} \end{bmatrix} \tag{5}$$

with $\boldsymbol{\lambda}$ is the vector of Lagrange multipliers, and $\mathbf{f}_c = \mathbf{A}^T\boldsymbol{\lambda}$.

For redundantly constrained systems at least one of the kinematic constraints in Eq. (3) can be expressed as a linear combination of the others. In mathematical terms, this means that the Jacobian matrix $\mathbf{A}$ of the system does not have a full row rank. Under these conditions, the individual constraint forces associated with the constraint equations cannot be fully determined [33], only their resultant effect can be considered.

It may be worth at this point to discuss some more basic features related to the appearance of redundant constraints. The dynamic and kinematic equations we generally deal with give certain representations of physical systems. Such mathematical models can never be

considered as the absolute description of a physical system. They usually include some information about the system to capture required behaviours, but at the same time they cannot represent other phenomena. The presence of redundant constraints is usually an example of this. In such a situation, the system model does not include enough information to uniquely determine all the constraint reactions. A prime example for this in multibody dynamics is the case in which the system model is built up using rigid bodies and constraint equations to represent certain kinematic specifications. Each constraint is associated with a generalized constraint force that is represented with the corresponding Lagrange multiplier.[1] In a physical system no perfect constraints exist and the constraint forces generally correspond to load distributions within the system. Usually, the nature of such load distributions depends on the structural properties of the system. If these structural properties are not represented in the model, as in the case of rigid bodies, then the individual constraint reactions, the Lagrange multipliers, can be determined uniquely only in certain situations. These are the cases when the constraint Jacobian matrix has a full row rank, i.e., the kinetostatic equilibrium in the subspace of constrained motion can fully be resolved without accounting for the structural properties of the system.

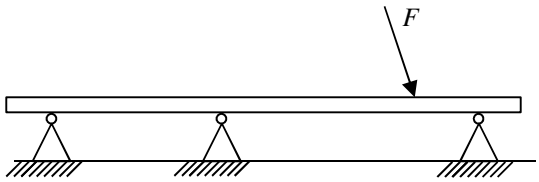

Fig. 1 A beam supported with three revolute joints is an example of a redundantly constrained mechanical system

Physically, this directly corresponds to the case of statics where we deal with statically determinate and indeterminate structures. If a structure is determinate, for example a simply supported beam or a cantilever beam, then the support reactions can be uniquely determined without the need to consider the deformation profile of the system. However, if the structure is indeterminate, for example a planar beam model with three supports (Figure 1), then material properties and strain-stress relationships of the structure need to be considered. In statics there are several methods available to resolve indeterminacy, for example via Castigliano's theorems.

If the constraint Jacobian does not have a full row rank then the only physically meaningful way to determine the Lagrange multipliers is to include the structural properties to represent the stiffness distribution in the system. The other possibility for the analysis is to consider the resultant effect of the constraint reactions. The Lagrange multipliers are not determined, but their resultant effect is represented with $\mathbf{f}_c = \mathbf{A}^{\mathrm{T}}\boldsymbol{\lambda}$. This $\mathbf{f}_c$ can be determined in the case of redundant constraints also, as was illustrated for example in [25] and [22]. In the case of redundantly constrained systems, $\mathbf{f}_c$ can be seen as the generalized constraint force resultant; it gives the representation of the constraint reactions with respect to the base vectors of the configuration space as defined by the selection of the generalized

[1] The physical unit and nature of the Lagrange multiplier is related to the associated constraint. For example, if the constraint equation is formulated in a way in which its unit is that of displacement, e.g. meters, then the unit of the associated generalized constraint force, the Lagrange multiplier, is Newton. The important relationship is that the time derivative of the constraint multiplied with its Lagrange multiplier must always result in a function with the unit of power.

coordinates and velocities. On the other hand, $\boldsymbol{\lambda}$ gives a representation of the constraint reactions with respect to the base vectors of the configuration space that are directly defined by the constraints.

Interestingly, the topic of redundant constraints and the algorithms that are able to handle such cases have received relatively little attention in the multibody literature. A considerable number of publications approaching the problem from a strictly kinematic point of view can be found, either proposing methods to compute the mobility of a mechanism (e.g. [21]) or discussing the physical meaning, applicability and limitations of the mobility formulas ([29], [27]). It has to be noted here that the concept of redundantly constrained system may be understood in different ways in kinematics and in dynamics. In kinematics, the focus is on the mobility formula that can give the right degree-of-freedom for the mechanism. Despite the existing research in kinematics, there is generally a lack of research material about the available techniques to deal with redundant constraints in dynamic simulations and analysis. A considerable number of publications in multibody dynamics simply assume that no redundant constraints are present and the leading matrix in Eq. (5) is invertible. For example the Schur complement method and the range space method described in [30], or the velocity and position projections for constraint violation suppression described in [8] are based on that assumption. A summary of different methods to deal with redundant constraints is found in [28], and results were reported in [33] and [16] on the identification of reaction forces uniquely determinable in the presence of redundant constraints. Recently, conditions for the existence and uniqueness of the solution of Eq. (5) were given in [18]. As discussed above, in the presence of redundant constraints, the accelerations $\ddot{\mathbf{q}}$ and the resultant generalized constraint forces, $\mathbf{f}_c = \mathbf{A}^{\mathrm{T}}\boldsymbol{\lambda}$, are uniquely defined, provided that $\mathbf{M}$ and $\boldsymbol{\Phi}$ have been adequately given. However, the particular reaction forces, as given by the Lagrange multipliers $\boldsymbol{\lambda}$, are not uniquely determined. In fact, there is an infinite set of solutions for $\boldsymbol{\lambda}$, that corresponds to the set of feasible reaction forces compatible with the motion of the system.

Determining the motion alone is often the primary goal of dynamic simulations and the precise determination of particular constraint reactions is not required, only their resultant effect is needed. In these cases, it is enough for the simulation algorithm to compute the accelerations and the resultant of the constraint reactions. This can be done with the use of reduction techniques [26] for example. However, if the particular reaction forces are of interest (e.g., when friction forces enter the picture or for design purposes), then the individual constraint reactions need to be determined to obtain a realistic solution. In the general case, this cannot be done without including additional information about the structural properties of the system. A possible solution is to use flexible bodies to represent components of the mechanism [35].

In this paper we will illustrate that, in some cases, penalty factors can be used in conjunction with natural coordinates as alternative to flexible body models in order to capture the effect of stiffness distribution in the system. Natural coordinates model each body in the system with a set of points and vectors, bound together by kinematic constraint equations representing the rigid body assumption. It is possible to relax these rigid body constraints by associating a penalty factor to each of them. In the literature often a single penalty factor α is assigned to all the constraint equations. The penalty factor is then considered just as an "arbitrarily large number". However, an adequate scaling of the penalty factors $\alpha_k = \eta_k \alpha$ for each constraint equation $\Phi_k = 0$ can be used to approximate the structural properties and the stiffness distribution of the system, and obtain accurate values of the constraint reactions in an efficient way.

This paper aims at the development of a methodology to use the penalty factors, already present in the augmented Lagrangian formulations, as a means to model the structural properties of mechanical systems. This technique can be applied in a straightforward fashion in many cases, hence providing an efficient and easy implementation to estimate and compute individual constraint reactions in redundantly constrained system models.

The paper is structured as follows: Section 2 describes the physical meaning of the penalty factors, their interpretation in multibody dynamics, and the modelling in natural coordinates. The dynamic formulations used in this work are introduced in Section 3. The use of scaled penalty factors is discussed in Section 4 to compute the reaction forces, first for a simple example with known analytical solution and later for a more complex, non-trivial problem. Finally, the conclusions of the study are summarized in Section 5.

2 Physical Meaning of Penalty Factors

The use of penalty factors as a technique to enforce the satisfaction of kinematic constraints with a Lagrangian formulation is described by Bayo et al. in [5]. We follow here their notation, according to which the integral action A of the mechanical system, including the effect of the constraint equations via the use of the Lagrange multipliers, is

$$A = \int_{t_1}^{t_2} L dt + \int_{t_1}^{t_2} W dt + \int_{t_1}^{t_2} \sum_k \lambda_k \Phi_k dt \tag{6}$$

where W represents the action of the nonconservative forces, and L is the system Lagrangian. In the proposed formulation, for the case of holonomic constraints, the last element in Eq. (6) is replaced by employing three additional terms representing a fictitious potential

$$V^* = \sum_k \frac{1}{2} \alpha_k \omega_k^2 \Phi_k^2 \tag{7}$$

a set of dissipative forces

$$G_k = -2\alpha_k \omega_k \mu_k \frac{d\Phi_k}{dt} \tag{8}$$

and a fictitious kinetic energy term

$$T^* = \sum_k \frac{1}{2} \alpha_k \left(\frac{d\Phi_k}{dt} \right)^2 \tag{9}$$

The additional terms introduced in Eqs. (7) – (9) give the representation of kinematic constraint Φ_k by a penalty system, with natural frequency ω_k and damping ratio μ_k. Similar expressions can be found for systems involving nonholonomic constraints. The modified action A then becomes

$$A^* = \int_{t_1}^{t_2} L dt + \int_{t_1}^{t_2} W dt + \int_{t_1}^{t_2} \sum_k \left[\frac{1}{2} \alpha_k \left(\frac{d\Phi_k}{dt} \right)^2 + G_k \Phi_k - \frac{1}{2} \alpha_k \omega_k^2 \Phi_k^2 \right] dt \tag{10}$$

The imposition of the condition $\delta A^* = 0$ yields

$$\mathbf{M}\ddot{\mathbf{q}} = \mathbf{f}_a - \mathbf{c} + \mathbf{A}^{\mathrm{T}} \boldsymbol{\Xi} \left(\ddot{\boldsymbol{\Phi}} + 2\boldsymbol{\Omega}\mathbf{N}\dot{\boldsymbol{\Phi}} + \boldsymbol{\Omega}^2 \boldsymbol{\Phi} \right) \tag{11}$$

where $\boldsymbol{\Xi}$, $\mathbf{N}$ and $\boldsymbol{\Omega}$ are penalty matrices, that contain the values of α_k, μ_k and ω_k for the different constraint equations. The fictitious potential in Eq. (7), as originally defined in [5], does not account for coupling between the different constraints. In that case, these matrices are diagonal. For example, $\boldsymbol{\Xi}$ can be expressed as

$$\boldsymbol{\Xi} = \begin{bmatrix} \alpha_1 & 0 & \cdots & 0 \\ 0 & \alpha_2 & \cdots & 0 \\ \vdots & \vdots & \ddots & \vdots \\ 0 & 0 & \cdots & \alpha_m \end{bmatrix} = \alpha \begin{bmatrix} \eta_1 & 0 & \cdots & 0 \\ 0 & \eta_2 & \cdots & 0 \\ \vdots & \vdots & \ddots & \vdots \\ 0 & 0 & \cdots & \eta_m \end{bmatrix} = \alpha \mathbf{H} \tag{12}$$

so the different penalty factors can be seen as a single penalty factor multiplied with a proportionality factor η_k for each constraint equation. Matrices $\boldsymbol{\Omega}$ and $\mathbf{N}$ can be treated in a similar way, allowing for the definition of different natural frequencies and damping parameters in each constraint equation. Alternatively, it is possible to define the fictitious potential V^* in a way in which stiffness coupling among the different constraints is introduced. Following this approach, non-zero off-diagonal values would appear in Eq. (12).

Eq. (11) is the starting point for a number of penalty and augmented Lagrangian formulations (e.g. [6], [12] [20]). All of them have in common that the kinematic constraints that define the motion of the system are relaxed and replaced by mass-damper-spring systems, introduced through the addition of the extra terms in Eq. (11). As shown by Eqs. (10) – (12), the penalty factors α_k, as well as terms μ_k and ω_k, can be different for each constraint. The possibility of scaling the penalty factors is already implied in [5]. However, for a wide range of purposes, the use of single scalar values for α, μ and ω in every constraint equation is an acceptable solution, and it is frequently found in the literature (e.g. [14], [24]). If all the constraint equations defined by $\boldsymbol{\Phi} = \mathbf{0}$ are linearly independent, then the Jacobian matrix $\mathbf{A}$ has full row rank, and Eq. (6) has a unique solution for both the accelerations $\ddot{\mathbf{q}}$ and the particular reaction forces $\boldsymbol{\lambda}$ [18]. Even in the case where redundant constraints are present $\mathbf{A}^{\mathrm{T}}\boldsymbol{\lambda}$ can be uniquely determined. In this case, when the motion of the system is the only required output and no forces are dependent on the particular reactions (such as in the case of friction), a single value of the penalty factor will yield the expected motion of the system, despite the multiplicity of feasible solutions for $\boldsymbol{\lambda}$. In these cases, the penalty factor α is frequently regarded as an arbitrarily large number ([6], [34]) which can actually be modified, for example, to improve the convergence properties.

The effect of the magnitude and the scaling of penalty factors on the stability and accuracy of dynamic simulations were studied in [4], [3] and [2]. On the other hand, interpretations of the physical meaning of the penalty factors were reported in [20] and [7]. The second of these papers stresses the meaning of the terms α_k, μ_k and ω_k as inertia, damping and stiffness coefficients, and the fact that these are not dimensionless quantities, but they have physical units. Nevertheless, the ability of the penalty technique to model the structural properties of a mechanism has not been discussed yet, nor it has been applied to the computation of reaction forces in redundantly constrained multibody systems.

2.1 Modelling Rigid Bodies using Natural Coordinates

Natural coordinates [19] have been used in several fields such as biomechanics, flexible multibody systems or real-time simulation [17]. A main advantage of these coordinates is that they result in a constant mass matrix, which needs to be computed only once at the beginning of the simulation. This eliminates the velocity dependent Coriolis and centrifugal

forces $\mathbf{c}$ from the equations of motion, simplifies the evaluation of the dynamic terms of the formulation and reduces the computational effort required.

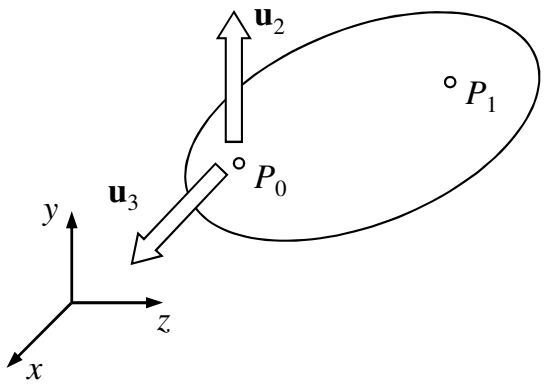

Fig. 2 A generic spatial rigid body, modelled with four natural coordinates: basic points P_0 and P_1 and basic vectors $\mathbf{u}_2$ and $\mathbf{u}_3$.

Using natural coordinates a body in the system is represented as a set of basic points and vectors, each of them defined by its global components, with associated inertia properties and constraints. Modelling in natural coordinates requires a minimum of four non co-planar basic points[2] per body in order to obtain a constant mass matrix of the system. The relative position between these elements is kept constant via the addition of kinematic constraints that transform the set of points and vectors into a rigid entity. In the example shown in Figure 2, six constraints are required to ensure rigid body behaviour. First the distance between the two basic points $P_0\,(x_0, y_0, z_0)$ and $P_1\,(x_1, y_1, z_1)$ is kept constant with a distance constraint

$$\Phi_1 = \frac{(x_1 - x_0)^2 + (y_1 - y_0)^2 + (z_1 - z_0)^2}{L} - L = 0 \tag{13}$$

where L is the reference distance between the two points. The angle between vectors $\mathbf{u}_2 = [x_2, y_2, z_2]^{\mathrm{T}}$ and $\mathbf{u}_3 = [x_3, y_3, z_3]^{\mathrm{T}}$ has to be constant too. This is achieved by constraining the scalar product of the two vectors to be constant, with the equation

$$\Phi_2 = x_2 x_3 + y_2 y_3 + z_2 z_3 - C = 0 \tag{14}$$

with C the value of the scalar product of the two vectors. Two more constant angle equations in the same form (Φ_3 and Φ_4) are introduced in order to maintain a constant angle between the direction defined by points P_0 and P_1 and vectors $\mathbf{u}_2$ and $\mathbf{u}_3$, respectively. Finally, other two constraint equations are necessary to keep the magnitude of vectors $\mathbf{u}_2$ and $\mathbf{u}_3$ constant and equal to 1.

The joints of the system can be modelled following a similar approach. When natural coordinates are used, revolute and spherical joints require two basic points that belong to two different bodies, $P_3\,(x_3, y_3, z_3)$ and $P_4\,(x_4, y_4, z_4)$, and share the same location in space during motion. A common way of enforcing this is simply defining one single point and sharing it between the two bodies. However, if the reaction forces at the joint are of interest, constraint equations with their corresponding Lagrange multipliers need to be defined. The

[2] Out of these four up to three may be replaced with basic vectors.

definition of both points P_3 and P_4 becomes necessary, and the three introduced constraint equations take the form

$$\begin{cases} \Phi_{j1} = x_4 - x_3 = 0 \\ \Phi_{j2} = y_4 - y_3 = 0 \\ \Phi_{j3} = z_4 - z_3 = 0 \end{cases} \tag{15}$$

The alignment between two vectors can be enforced in the same way. Alternatively, constant angle equations like (14) can be defined for joints too.

2.2 Constraint Reactions

In an augmented Lagrangian formulation, these above-mentioned rigid body and joint constraints are relaxed and the associated constrained dynamics is represented with penalty systems. This way, a penalty factor α_k is assigned to each of them. Based on this and according to Eq. (11), the Lagrange multiplier associated with constraint Φ_k will have the representation

$$\lambda_k = \alpha_k \left(\ddot{\Phi}_k + 2\omega_k \mu_k \dot{\Phi}_k + {\omega_k}^2 \Phi_k \right) \tag{16}$$

which can be interpreted as a generalized reaction force associated with the constraint, the magnitude of which is dependent on the violation of the constraint at the position, velocity and acceleration levels and also on parameters α_k, μ_k and ω_k. In order to make the reaction force proportional to the violation of the constraints at position level, parameters μ_k and ω_k can be appropriately chosen. The value of μ_k is usually set to unity in order to ensure critical damping. Setting the value of ω_k to a value in the order of 10, which is a common practice [15], makes the contribution of the constraint violation at position level at least one order of magnitude greater than those at velocity and acceleration levels. In this case, it is admissible to consider that the reaction forces are proportional to $\alpha_k \Phi_k$, which can be seen to represent the assumption of linear stiffness behaviour for the violation of constraints. Accordingly, the constraint reactions be expressed as a function of the violation of the constraints at position level as

$$\boldsymbol{\lambda} = \boldsymbol{\Xi} \boldsymbol{\Phi} = \alpha \mathbf{H} \boldsymbol{\Phi} \tag{17}$$

The modification of α within stability margins does not change the solution of Eq. (11), for the accelerations and generalized constraint forces $\mathbf{A}^{\mathrm{T}} \boldsymbol{\lambda}$. It was shown in [9] that the solution of Eqs. (6) and (10) converges to the same values, both for $\ddot{\mathbf{q}}$ and $\boldsymbol{\lambda}$, when $\alpha \to \infty$. Accordingly, if matrix $\mathbf{H}$ is kept unchanged, a new value of α will result in a proportional change for the violation of constraints $\boldsymbol{\Phi}$, and will not influence the value of $\boldsymbol{\lambda}$. As a consequence, the distribution of the constraint reactions is governed by the interrelationships and proportions among the stiffness values associated with the constraints. The nature of the stiffness distribution is characterized by $\mathbf{H}$. The numerical value of the global penalty factor α does not influence the constraint reactions.

We can further illustrate this concept. Let us assume that a multibody system is subjected to m constraints, of which r are redundant. Therefore, these m constraints restrict the motion of the system in an $m - r$ dimensional subspace, the constrained motion subspace. The m constraint reactions are represented with an $m \times 1$ array $\boldsymbol{\lambda}$. From basic analysis of force systems we know that the resultant effect of these reactions on the constrained motion can be represented with $m - r$ resultant components that can be given in an $(m - r) \times 1$ array $\mathbf{g}$. This resultant can be expressed as $\mathbf{g} = \mathbf{D}\boldsymbol{\lambda}$, where $\mathbf{D}$ is an $(m - r) \times m$ full row rank matrix

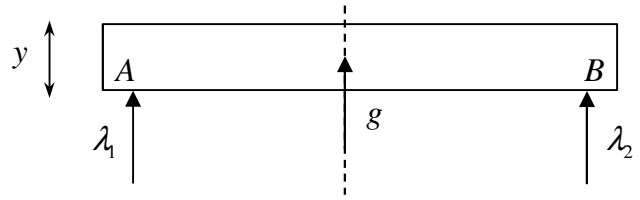

Fig. 3 Schematic representation of two constraints associated with the same generalized direction of a multibody system.

that is determined by the design of the mechanical elements that realize the constraints of the system at hand.

The resultant of the constraint reactions, $\mathbf{g}$, is determined by the state of the overall multibody system for any instant [25]. Considering Eq. (17), where the constraint violations $\mathbf{\Phi}$ can represent the displacements in the constrained motion subspace, $\mathbf{g}$ can be expressed as

$$\mathbf{g} = \alpha \mathbf{D}\mathbf{H}\mathbf{\Phi} \tag{18}$$

where $\mathbf{g}$ is uniquely determined for a given motion of the system. Matrices $\mathbf{D}$ and $\mathbf{H}$ are also set by the design of the system and the stiffness representation in the constrained motion subspace. Based on this we can see that if α is increased or decreased then $\mathbf{\Phi}$ needs to change proportionally in the opposite sense so that the $\alpha\mathbf{\Phi}$ product will always remain the same. This can be understood also based on the principles of structural mechanics. If a structure is subjected to a given load and the nature of the stiffness distribution in the system is set, then rescaling the stiffness values with a single multiplier will induce a proportional change in the resulting displacement and strain fields of the structure[3].

A simple illustration of the above can be the case depicted in Figure 3, where the constrained motion subspace is one–dimensional, represented with coordinate y, and the motion is constrained via the introduction of two forces, λ_1 and λ_2. The resultant of these two forces is g. In this case,

$$\mathbf{\Phi} = \begin{bmatrix} \phi_1 & \phi_2 \end{bmatrix}^{\mathrm{T}} \; ; \qquad \mathbf{D} = \begin{bmatrix} 1 & 1 \end{bmatrix} \tag{19}$$

and

$$\mathbf{H} = \begin{bmatrix} k_1 & 0 \\ 0 & k_2 \end{bmatrix} \tag{20}$$

where $\phi_1 = y$ and $\phi_2 = y$ represent the constrained displacements of points A and B, and k_1 and k_2 are the stiffness values associated with λ_1 and λ_2, respectively. Based on the above formulation, simple hand calculation shows that, once g is set, the values of λ_1 and λ_2 only depend on the ratio between k_1 and k_2; they do not depend on the selected value of α.

Eq. (17), however, does not represent the general case for the value of Lagrange multipliers, as shown in [18]. The value of the generalized constraint forces remains the same if a vector $\boldsymbol{\lambda}_0$ that belongs to the nullspace of $\mathbf{A}^{\mathrm{T}}$ is added to the particular reaction forces. In this case

$$\boldsymbol{\lambda}^* = \boldsymbol{\lambda}_0 + \mathbf{\Xi}\mathbf{\Phi} = \boldsymbol{\lambda}_0 + \boldsymbol{\lambda}_1 \tag{21}$$

[3] We assumed here that the behaviour of the structure can be well represented with the small displacement – small strain assumption.

but the effective generalized constraint forces are not affected,

$$\mathbf{f}_c^* = \mathbf{A}^{\mathrm{T}} \left(\boldsymbol{\lambda}_0 + \boldsymbol{\Xi}\boldsymbol{\Phi} \right) = \mathbf{A}^{\mathrm{T}} \boldsymbol{\lambda}_0 + \mathbf{A}^{\mathrm{T}} \boldsymbol{\lambda} = \mathbf{A}^{\mathrm{T}} \boldsymbol{\lambda} = \mathbf{f}_c \tag{22}$$

as $\mathbf{A}^{\mathrm{T}} \boldsymbol{\lambda}_0 = \mathbf{0}$ because $\boldsymbol{\lambda}_0$ belongs to the nullspace of $\mathbf{A}^{\mathrm{T}}$. The term $\boldsymbol{\lambda}_0$ can correspond to a set of self-balancing reaction forces that do not modify $\mathbf{f}_c$ during the motion. These forces are determined by the configuration of the mechanism, the loads and the stiffness distribution of the system. For example, this term can represent pre-loads in the mechanical system, due to pre-stressing, assembly defects or thermal stresses. It is possible to obtain $\boldsymbol{\lambda}_1$ at each time step in the simulation for the unloaded system ($\boldsymbol{\lambda}_0 = \mathbf{0}$), computing the value of $\boldsymbol{\lambda}_0$ in parallel with the main simulation, and to superimpose the two load scenarios to obtain $\boldsymbol{\lambda}^* = \boldsymbol{\lambda}_0 + \boldsymbol{\lambda}_1$. Alternatively, these can be considered in the dynamic simulation of the system by introducing the corresponding term $\boldsymbol{\lambda}_0$ in Eq. (17). For example, in the augmented Lagrangian formulation described in Section 3, $\boldsymbol{\lambda}_0$ can be taken as the initial value for the iterative process used in the computation of the Lagrange multipliers.

It is noteworthy that this technique for the determination of the constraint reactions implies that the violation of the kinematic constraints at position level is negligible when compared to the displacements occurring during the motion of the system. The configuration of the system is not modified by the consideration of flexibility. The effects of structural flexibility are taken into consideration only to determine the reaction force distributions. In other words, the use of structural properties to determine the reactions does not add any new coordinates to the system, and the configuration space of the system remains the same. This represents an important difference with respect to modelling the components of the system as flexible bodies (e.g. [1], [10]). In that case new additional coordinates are explicitly introduced to represent the deformation field of the bodies, and the model of the system is altered via changing its configuration space.

3 Dynamic Formulations

Two dynamic formulations have been employed in this paper to carry out the forward dynamic simulations. The method of the scaling of penalty factors to model the distribution of structural stiffness is tested using an augmented Lagrangian formulation of index-3 with mass-orthogonal projection of velocities and accelerations. The index-3 formulation is described by Cuadrado et al. [12]. With this formulation, the dynamic equations of a multibody system are represented in the form:

$$\begin{aligned} &\mathbf{M}\ddot{\mathbf{q}} - \mathbf{A}^{\mathrm{T}}\boldsymbol{\Xi}\boldsymbol{\Phi} - \mathbf{A}^{\mathrm{T}}\hat{\boldsymbol{\lambda}} = \mathbf{f}_a \\ &\hat{\boldsymbol{\lambda}}^{j+1} = \hat{\boldsymbol{\lambda}}^{j} + \boldsymbol{\Xi}\boldsymbol{\Phi}^{j+1}; \quad j = 0, 1, 2, ... \end{aligned} \tag{23}$$

The penalty matrix $\boldsymbol{\Xi}$ in Eq. (23) is actually the product of matrices $\boldsymbol{\Xi}$ and $\boldsymbol{\Omega}^2$ in Eq. (11). Matrix $\boldsymbol{\Omega}^2$ introduces only an additional scaling to the matrix of penalty factors, in the same way as $\mathbf{H}$ does, so the notation $\boldsymbol{\Xi}$ will be used to denote this product for the sake of clarity. The algorithm incorporates the equations of the numerical integrator in the solution process of Eqs. (23) through a Newton-Raphson iteration. The Lagrange multipliers for each time step are also updated during this iterative process. The initial value of $\hat{\boldsymbol{\lambda}}^0$ is set to the value of the multiplier obtained in the previous time step. The contribution of the penalty damping and inertia terms to the Lagrange multipliers is neglected, because the violation of constraints at velocity and acceleration levels is removed by the projection of velocities and

accelerations at the end of each integration time step. This formulation has shown very good efficiency and robustness properties for a wide range of applications (e.g. [24], [13], [23]).

A second dynamic formulation, based on the use of the Moore-Penrose generalized inverse, is used for comparison in the subsequent tests. It is possible to directly solve Eq. (5) using a generalized inverse [34]. Similar formulations, also based on the use of minimum norm solution and generalized inverses can be found in [28], and [31], among others. After including some additional terms for the stabilization of the constraints at position and velocity levels, this leads to

$$\begin{bmatrix} \ddot{\mathbf{q}} \\ \boldsymbol{\lambda} \end{bmatrix} = \begin{bmatrix} \mathbf{M} & -\mathbf{A}^{\mathrm{T}} \\ -\mathbf{A} & \mathbf{0} \end{bmatrix}^{\dagger} \begin{bmatrix} \mathbf{f}_a \\ \dot{\mathbf{A}}\dot{\mathbf{q}} + \dot{\mathbf{b}} + 2\xi\omega\dot{\boldsymbol{\Phi}} + \omega^2\boldsymbol{\Phi} \end{bmatrix} \tag{24}$$

where symbol † stands for the Moore-Penrose generalized inverse.

Although it is not a numerical formulation, the removal of redundant constraints from Eqs. (5), either manually or automatically, is a commonly used way of eliminating the indeterminacy present in overconstrained systems. This strategy replaces the original system with a kinematically equivalent one. It sometimes requires the use of additional algorithms to decide which constraint equations are to be removed. The results obtained following this approach are shown for comparison when discussing the reaction forces for the examples in Section 4.

3.1 Generalization of the Index-3 Augmented Lagrangian Algorithm

So far we have followed the usual augmented Lagrangian formulation as was originally derived in [5]. However, the penalty terms in (6) can also be reformulated in a slightly different way to include a more general representation for structural stiffness. The potential energy part in (7) can be stated in a general form as

$$V^* = \frac{1}{2}\boldsymbol{\Phi}^T\mathbf{K}_c\boldsymbol{\Phi} \tag{25}$$

where $\mathbf{K}_c$ is the stiffness matrix for the constrained motion of the system. Such a stiffness matrix can be found via considering the effective structural stiffness properties in the constrained motion space. For example, for natural coordinates such stiffness matrices were discussed in [11] for flexible multibody modelling.

Using this above potential energy expression Eq. (23) can be rewritten as

$$\begin{aligned} &\mathbf{M}\ddot{\mathbf{q}} - \mathbf{A}^{\mathrm{T}}\alpha\mathbf{K}_c\boldsymbol{\Phi} - \mathbf{A}^{\mathrm{T}}\hat{\boldsymbol{\lambda}} = \mathbf{f}_a \\ &\hat{\boldsymbol{\lambda}}^{j+1} = \hat{\boldsymbol{\lambda}}^{j} + \alpha\mathbf{K}_c\boldsymbol{\Phi}^{j+1}; \quad j = 0, 1, 2, ... \end{aligned} \tag{26}$$

where α is the penalty factor. Based on this the original algorithm can be reformulated for the more general case replacing matrix $\boldsymbol{\Xi}$ with $\alpha\mathbf{K}_c$. In this new formulation the role of the scaling factors, η_k, is replaced by $\mathbf{K}_c$ that represents the nature of stiffness distribution associated with the constraints.

4 Test Problems

In order to demonstrate the use of penalty factors as a means to model the structural properties of a redundantly constrained system, a simple pendulum, shown in Figure 4 was chosen as first example. The pendulum consists of a point mass $m = 1$ kg attached to the end of a massless rod of length $l = 2$ m, and moving under the effect of gravity. The three-dimensional model of the pendulum is composed of a set of natural coordinates including the coordinates of points O and P and the components of vectors $\mathbf{u}_1$ and $\mathbf{u}_2$. Vector $\mathbf{u}_2$ is perpendicular to the rod along the z axis and $\mathbf{u}_1$ is perpendicular to both the rod and $\mathbf{u}_2$. A revolute joint at point O constrains the motion of the pendulum to the $x - y$ plane. In the initial configuration, $\theta = 0$ and all the velocities are zero.

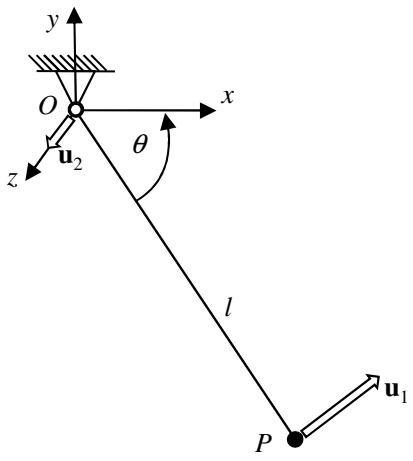

Fig. 4 Simple planar pendulum

The system has one degree of freedom, and out of the 12 natural coordinates used in the modelling (three for each basic point or vector), six are constrained to be constant due to the revolute joint at O (i.e., the ones corresponding to point O and vector $\mathbf{u}_2$). The rigid body nature of the pendulum is modelled with one constant distance equation between points O and P, three constant angle equations between vectors $\mathbf{u}_1$, $\mathbf{u}_2$ and axis O–P, and an additional constraint imposing that the norm of vector $\mathbf{u}_1$ is constant and equal to 1 (such a constraint is not required for $\mathbf{u}_2$, as its value does not change during motion, by effect of the revolute joint). These 11 independent constraints mean that, out of the 12 natural coordinates, only one is independent. The Jacobian matrix $\mathbf{A}$ of the system is full row rank, and the system is not redundantly constrained, so its motion and the reaction forces can be computed using any of the algorithms available in the literature. In this particular case, the reaction force developed in rod O–P can also be computed as

$$F = m\dot{\theta}^2 l - mg\sin\theta \tag{27}$$

In the formulation with natural coordinates, this reaction force corresponds to the constraint force of the constant distance constraint between the points O and P representing the rod.

If a second rod is added to the pendulum between points O and P, a new constant distance constraint is introduced, leading to a redundantly constrained system. As a consequence, the Jacobian matrix $\mathbf{A}$ becomes rank deficient and Eq. (5) needs to be solved using

algorithms able to deal with redundant constraints such the ones described in Section 3. All these algorithms (removal of redundant constraints, use of generalized inverse techniques, penalty factors) correctly find the uniquely determined accelerations of the system, $\ddot{\mathbf{q}}$. However, they differ in the determination of the particular reaction forces. The reaction force F will be now shared between the two rods. If the rods have linear stiffness characteristics, the load corresponding to each one will be proportional to its stiffness. Removing the redundant constraint equations introduced by the second rod transfers all the reaction load to the remaining rod, which would not represent the physics of the system correctly. An alternative is to use a single penalty factor α for all the constraint equations, or another possibility is to solve Eq. (5) with the generalized inverse formulation. For the present system, these two techniques give the same solution. This solution corresponds to the minimum norm one, and is equivalent to distribute uniformly the reaction force among the two rods. However, none of these solutions consider the structural properties of the system which, ultimately, will determine the actual value of the reactions. In this case, the use of scaled penalty factors allows for the inclusion of these properties in the computation of the reaction forces in a simple way. For example, in the case in which the stiffness of one of the rods is the double of the other, the relative scaling factors for the two constant distance equations Φ_1 and Φ_2 corresponding to each link can be set to $\eta_2 = 2\eta_1$ to model the relation between the stiffness properties of the bars. It has to be noted here that the axial stiffness distribution of the rods is the only physical parameter influencing the axial force distribution. This illustrates two facts. In the first place, the scaling factors corresponding to the other constraint equations do not affect the results regarding axial loads. Secondly, it is the proportion between stiffness parameters, and not the particular numerical values of them, that determines the reaction forces developed.

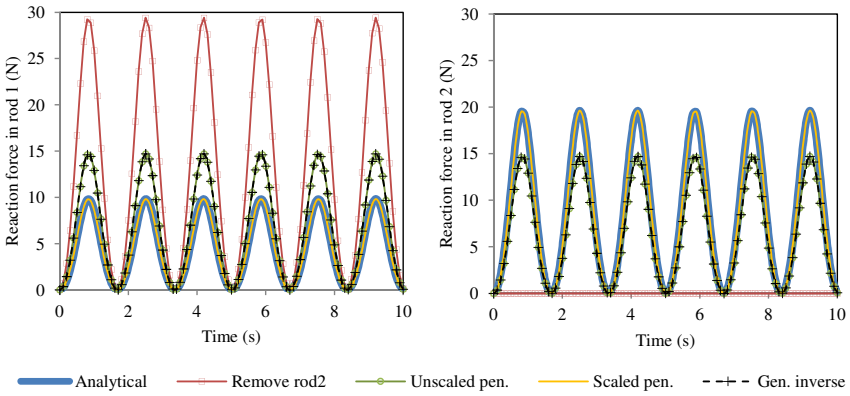

Fig. 5 Reaction forces in rods 1 (left) and 2 (right) of the redundantly constrained simple pendulum

The scaling of penalty factors was tested in a 10 s long forward dynamic simulation of the motion of the pendulum, employing an augmented Lagrangian formulation of index-3 described in Section 3, and with an integration time step $h = 10^{-3}$ s. The common penalty factor α of Eq. (12) was set to $\alpha = 10^{10}$. The scaling factors η_k were assigned unit values, except for the constant distance equations corresponding to rods 1 and 2, which were set to $\eta_1 = 1{\cdot}10^{-3}$ and $\eta_2 = 2{\cdot}10^{-3}$. This represents a stiffness constant of $k_1 = 1{\cdot}10^{7}$ N/m and $k_2 = 2 \cdot 10^{7}$ N/m for the rods. The reaction forces thus obtained are compared in Figure 5

to the ones given by the alternative methods, namely the same formulation without scaling of penalties and removing the constraint equations corresponding to the second rod, and the generalized inverse solution also described in Section 3. The solution obtained using scaled penalty factors yields the value of the reaction forces predicted by the analytical solution. The use of techniques that do not consider the structural properties of the system gave solutions which are still compatible with the motion, but they do not produce the correct reaction force distribution.

The same simulation was repeated for two additional variations in the values of the penalty factors. In the first place, the value of the global penalty factor α was modified from $\alpha = 10^6$ to $\alpha = 10^{12}$. Secondly, the scaling factors η_1 and η_2 were altered, without changing the ratio between them, from 10^{-3} to 10^{-1}. No significant changes were obtained for the motion or reaction forces, which confirms that the proportion between the scaling factors is the only parameter that actually determines the magnitude of the reaction forces. Although, obviously, for numerical reasons, the value of the penalty factors must be kept in a range that does not compromise the stability of the numerical integration or the precision of the results.

In a second stage, the same forward dynamic simulation was carried out with a single-rod pendulum and introducing an additional joint at point O. This model can represent a configuration of the mechanism in which the rod is joined to the ground via two parallel bearings. In this case, the redundancy comes from an additional joint, instead of from a redundant link. The radial stiffnesses of the two joints were considered to be related by a ratio of 2:1. The reaction forces at each joint during motion were computed and they were found to be identical to the ones shown in Figure 5.

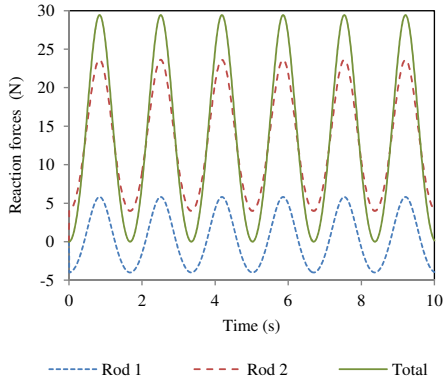

Fig. 6 Reaction forces for redundantly constrained simple pendulum under a pre-load of ± 4 N.

Finally, the motion of the system was simulated again as in the first case, but considering that the first rod was $6 \cdot 10^{-7}$ m longer that its nominal length. This caused a pre-load of -4 N in rod 1 and $+4$ N in rod 2, which was introduced in $\hat{\boldsymbol{\lambda}}^0$ in Eq. (23). The obtained results, displayed in Figure 6 agreed with the analytical solution: the reaction force in each rod was shifted a value of ± 4 N while the total force was left unchanged.

As a more complex example, we employed scaled penalty factors to approximate the structural properties of a spatial parallelogram mechanism (Figure 7), a detailed descrip-

tion of which can be found in [33] and [35]. In [35], the authors deal with the redundant constraints by replacing rigid body components with flexible ones.

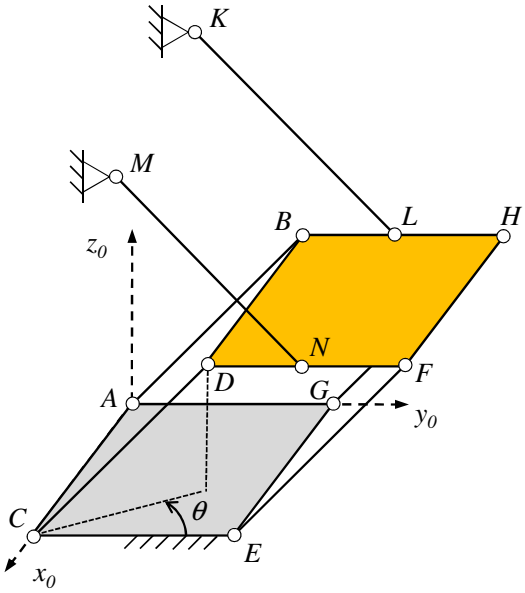

Fig. 7 Spatial parallelogram

The spatial parallelogram of Figure 7 consists of six rods of length $l = \sqrt{2}/2$ m, and a plate of size 0.5×0.5 m, linked via spherical joints to each other and to the ground. The inertial properties of the bodies are summarized in Table 1.

Table 1 Inertial properties (in local axes) of the spatial parallelogram

	mass [kg]	I_x [kg · m^2]	I_y [kg · m^2]	I_z [kg · m^2]
rod	0.34	$56 \cdot 10^{-3}$	$56 \cdot 10^{-3}$	$0.08 \cdot 10^{-3}$
plate	39.0	3.25	6.5	3.25

The system has 7 degrees of freedom: the plate can move horizontally, in parallel with the plane xy, and each rod can rotate freely about its longitudinal axis. The modelling of the parallelogram in natural coordinates required the definition of the 12 basic points depicted in Figure 7, plus two basic vectors per rod to obtain an adequate representation of each body with natural coordinates. An additional point and a vector perpendicular to the plate were added to simplify the application of the forces acting on the center of the plate. Moreover, three more points were attached to joints G, K, and M, to allow for the computation of the reaction forces. This resulted in a total of 29 basic points or vectors (each of them composed of three coordinates), of which 6 are constantly attached to the ground, so only 23 enter the formulation, leading to $n = 69$ generalized coordinates being used to model the system.

The number of constraint equations was $m = 63$, at least one of which is redundant. In [35], it was shown by the authors that the reaction forces in joints K and M can be uniquely determined, whereas the redundancy of constraints results in multiple solutions regarding the reactions at points A, C, E and G and the axial loads of the rods connected to them. The axial load of every rod is associated with the constant distance equation between the two points located at its ends. This force corresponds to the reaction at the joints in the axial direction of the bar.

The mechanism moves under gravity effects, with an external force applied to the center of the plate $\mathbf{f} = [2000, 3000, 3000]^{\mathrm{T}}$ N, and a torque $\boldsymbol{\tau} = [300, 0, 500]^{\mathrm{T}}$ Nm, acting on the same body, both expressed with respect to the global axes x_0, y_0, z_0. Initially, all the velocities are zero and $\theta = 0$. The initial positions of the points of the mechanism are given in Table 2.

Table 2 Positions of the joints (m) at the start of the motion, in the global axes x_0, y_0, z_0

	x	y	z		x	y	z		x	y	z
A	0.0	0.0	0.0	E	0.5	0.5	0.0	K	0.0	0.25	1.0
B	0.0	0.5	0.5	F	0.5	1.0	0.5	L	0.5	0.75	0.5
C	0.5	0.0	0.0	G	0.0	0.5	0.0	M	0.5	0.25	1.0
D	0.5	0.5	0.5	H	0.0	1.0	0.5	N	0.25	0.75	0.5

Every rod in the mechanism is a hollow aluminum cylinder, with inner and outer diameters $d_i = 0.028$ m and $d_o = 0.03$ m. The Young modulus of the material is $E = 6.9 \cdot 10^{10}$ Pa and the computation of the axial stiffness of the rod yields a value of $k = 8.89 \cdot 10^6$ N/m. In our model, the rods are considered to be flexible only in their axial direction, while all the other components are taken as rigid.

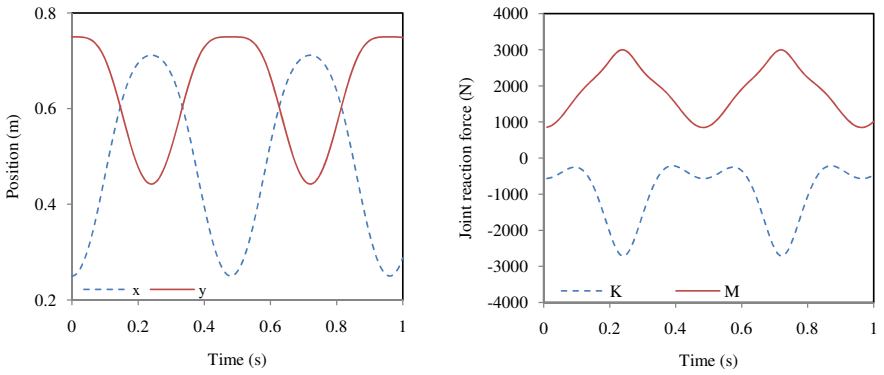

Fig. 8 Position of the center of mass of the upper platform (left), and axial reaction forces in joints K and M (right), during motion of the spatial parallelogram

A 1 s long forward dynamic simulation was carried out to compute the motion and constraint forces of the parallelogram. Here, the augmented Lagrangian formulation of index-3

with projections introduced in Section 3 was employed again to solve Eq. (5) for this problem. The selected integration time step was $h = 10^{-3}$ s. The global penalty factor was set to $\alpha = 8.89 \cdot 10^6$, to model the axial stiffness of the bars. The scaling factors η_k corresponding to the constant distance equations imposed by the rods were set to one, while those corresponding to every other constraint were set to values three orders of magnitude greater. As expected, the motion of the parallelogram and the computed axial reaction forces for the rods connected to joints K and M (Figure 8) matched those obtained via the use of flexible body models to represent the rods and plate of the mechanism in [35].

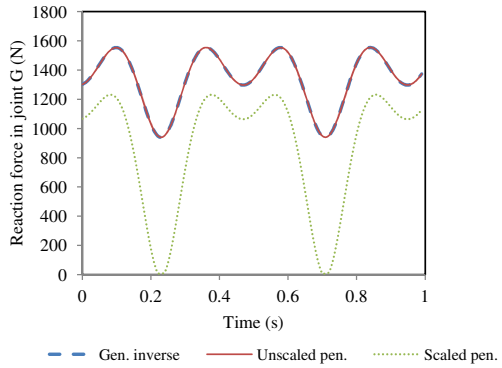

Fig. 9 Axial component of reaction in joint G during motion of the spatial parallelogram, computed with different techniques

The reactions in joints A, C, E and G, however, cannot be determined without considering the structural properties of the mechanism. It was found that the use of a generalized inverse and unscaled penalty factors resulted in the same reaction forces at these joints. The use of scaled penalty factors, on the other hand, gave the same results as the use of flexible body models employed in [35]. Results for the axial reaction at joint G are summarized in Figure 9. This is the component corresponding to the constant distance constraint acting between the two tips of the rod. The computed reaction forces clearly vary for the different methods and the minimum norm solution produced by the unscaled methods cannot be considered reliable for the general case.

Moreover, it was confirmed that the scaling relation between the different penalty factors is of critical importance for the accuracy of the results, whereas the numerical value of the penalty factor α has a much less noticeable impact. The same dynamic simulation was repeated increasing the value of the global penalty factor α one and two orders of magnitude, and the impact on the computed reaction forces was negligible (Figure 10).

These results also show that the penalty factors in matrix $\boldsymbol{\Xi}$ do not need to model the structural properties of the different components of the system down to exact numerical values.

Results in Figures 9 and 10 were obtained via scaling the penalty factors corresponding to the constant distance equations between the tips of the rods to three orders of magnitude smaller than the rest. This is equivalent to consider that the only relevant flexibility contributions in the mechanism are associated to the axial directions of the rods. Figure 11 shows the evolution of the reaction force at joint G when the proportion between the different penalty

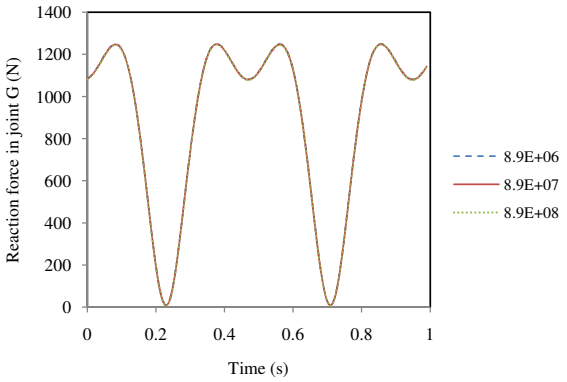

Fig. 10 Axial reaction forces in joint G during motion of the spatial parallelogram, computed with scaled penalties and different values of the global penalty factor α

factors is made closer to one. The case in which the ratio is one is equivalent to having unscaled penalty factors. A ratio of 100 was enough to obtain realistic results. However, it is difficult to extend the validity of this threshold for the general case. The nature of the constraint equations that can be used to model a mechanical system is very diverse. Some of them represent unit norms of vectors, other constant distances and other constant angles. The units in which the constraint equations are expressed can vary too. The scaling of the penalty factors needs to be studied according to the definition of the constraint equations in each problem.

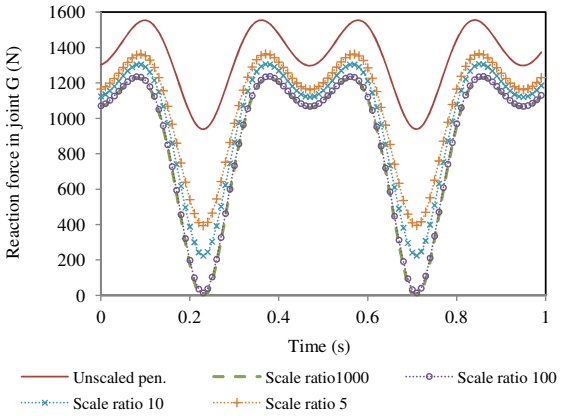

Fig. 11 Axial reaction forces in joint G during motion of the spatial parallelogram, computed with different ratios between the penalty factors associated with constant distance constraints and those associated with the rest

On the other hand, it can be stated that the stiffness distribution and the relationship among the different stiffness values are the decisive elements for the determination of the reaction forces. This relationship can be represented by the scaling factors contained in

matrix η, while the global penalty factor α can be modified to improve the stability or the efficiency of the computations.

5 Conclusions

Rigid multibody models of mechanical systems can lead to the existence of redundant kinematic constraints. In such a case, the individual reaction forces can only be determined if additional information about the structural properties of the system is included. One possibility for this is to change the system representation and consider a flexible multibody system model. In that case, additional new generalized coordinates are introduced together with the appropriate constitutive relations and the configuration space is enlarged to represent the new model. In this paper, we discussed that there is also another possibility. In this method the original rigid multibody model does not have to be changed. The structural properties are considered only to resolve the redundancy problem for the reaction forces. This can be achieved via the index-3 augmented Lagrangian penalty formulation. Index-3 augmented Lagrangian formulations have been employed in multibody system research for some years. However, they have been mostly used for motion simulation purposes where the accurate knowledge of the constraint reactions is not critical. In this work we illustrated that this formulation can also be used to resolve the redundancy problem for the constraint reactions. This results in a novel possibility to consider structural properties without changing the system model used for other simulation and analysis tasks the user has to consider. We also highlight that the use of natural coordinates can be particularly advantageous for this approach. These coordinates can be directly associated with the internal displacement field of a body, and as such, they result in stiffness representations for the penalty systems, which will remain valid as the system undergoes large configuration changes.

Our analysis shows that the use of penalty factors can provide an efficient and easy way to determine constraint reaction forces, as an alternative to employing flexible multibody models. Penalty factors in the index-3 augmented Lagrangian formulation are not meaningless large numbers, but they can be associated to significant physical quantities to represent the structural properties of the system. It should be stressed that a meaningful relation between the structural properties of the bodies and the definition of the constraint equations (which, in turn, determine the physical meaning of the penalty factors) has to be found for the modelling of the system. Once this relation is adequately defined, the value of the penalty factors can be adjusted to model the stiffness distribution in the system which is dominant for the development of the constraint reactions.

Acknowledgements This research was supported by the Natural Sciences and Engineering Research Council of Canada (NSERC), CMLabs Simulations Inc., and the Canadian Space Agency (CSA). The support is gratefully acknowledged.

References

1. Aarts, R.G.K.M., Meijaard, J.P., Jonker, J.B.: Flexible multibody modelling for exact constraint design of compliant mechanisms. Multibody System Dynamics **27**(1), 119–133 (2012)
2. Bauchau, O.A.: Parallel computation approaches for flexible multibody dynamics simulations. Journal of the Franklin Institute – Engineering and Applied Mathematics **347**(1), 53–68 (2010)
3. Bauchau, O.A., Epple, A., Bottasso, C.L.: Scaling of constraints and augmented Lagrangian formulations in multibody dynamics simulations. Journal of Computational and Nonlinear Dynamics **4**(021007), 1–9 (2009)

4. Bauchau, O.A., Laulusa, A.: Review of contemporary approaches for constraint enforcement in multibody systems. Journal of Computational and Nonlinear Dynamics **3**(011005), 1–8 (2008)
5. Bayo, E., García de Jalón, J., Serna, M.A.: A modified Lagrangian formulation for the dynamic analysis of constrained mechanical systems. Computer Methods in Applied Mechanics and Engineering **71**(2), 183–195 (1988)
6. Bayo, E., Ledesma, R.: Augmented Lagrangian and mass–orthogonal projection methods for constrained multibody dynamics. Nonlinear Dynamics **9**(1-2), 113–130 (1996)
7. Blajer, W.: Augmented Lagrangian formulation: Geometrical interpretation and application to systems with singularities and redundancy. Multibody System Dynamics **8**(2), 141 – 159 (2002)
8. Blajer, W.: Methods for constraint violation suppression in the numerical simulation of constrained multibody systems – A comparative study. Computer Methods in Applied Mechanics and Engineering **200**(13–16), 1568 – 1576 (2011)
9. Carey, G.F., Oden, J.T.: Finite Elements: A Second Course. Prentice–Hall (1983)
10. Chamorro, R., Escalona, J.L., González, M.: An approach for modeling long flexible bodies with application to railroad dynamics. Multibody System Dynamics **26**(2), 135–152 (2011)
11. Cuadrado, J., Cardenal, J., García de Jalón, J.: Flexible mechanisms through natural coordinates and component synthesis: An approach fully compatible with the rigid case. International Journal for Numerical Methods in Engineering **39**(20), 3535–3551 (1996)
12. Cuadrado, J., Cardenal, J., Morer, P., Bayo, E.: Intelligent simulation of multibody dynamics: Space–state and descriptor methods in sequential and parallel computing environments. Multibody System Dynamics **4**(1), 55–73 (2000)
13. Dopico, D., Luaces, A., González, M., Cuadrado, J.: Dealing with multiple contacts in a human-in-the-loop application. Multibody System Dynamics **25**(2), 167–183 (2011)
14. Dopico, D., Naya, M.A., Lugrís, U., Cuadrado, J.: Performance of an energy-conserving algorithm for multi-body dynamics. Proceedings of the Institution of Mechanical Engineers, Part K: Journal of Multi-Body Dynamics **222**(3), 243–253 (2008)
15. Flores, P., Machado, M., Seabra, E.: A parametric study on the Baumgarte stabilization method for forward dynamics of constrained multibody systems. Journal of Computational and Nonlinear Dynamics **6**(011019), 1–9 (2011)
16. Frączek, J., Wojtyra, M.: On the unique solvability of a direct dynamics problem for mechanisms with redundant constraints and coulomb friction in joints. Mechanism and Machine Theory **46**(3), 312–334 (2011)
17. García de Jalón, J.: Twenty–five years of natural coordinates. Multibody System Dynamics **18**(1), 15–33 (2007)
18. García de Jalón, J.: Multibody systems made simple and efficient. In: ASME 2011 IDETC/CIE D'Alembert Award keynote (2011). URL http://mat21.etsii.upm.es/mbs/ASME2011/Washington2011.pdf
19. García de Jalón, J., Bayo, E.: Kinematic and Dynamic Simulation of Multibody Systems. The Real–Time Challenge. Springer–Verlag (1994)
20. García Orden, J.C., Ortega, R.A.: A conservative augmented Lagrangian algorithm for the dynamics of constrained mechanical systems. Mechanics Based Design of Structures and Machines **34**(4), 449–468 (2006)
21. Gogu, G.: Mobility of mechanisms: a critical review. Mechanism and Machine Theory **40**(9), 1068–1097 (2005)
22. González, F., Kövecses, J., Teichmann, M., Courchesne, M.: Techniques for the simulation of redundantly constrained multibody systems. In: Multibody Dynamics 2011 ECCOMAS Thematic Conference. Brussels, Belgium (2011)
23. González, F., Naya, M.A., Luaces, A., González, M.: On the effect of multirate co-simulation techniques in the efficiency and accuracy of multibody system dynamics. Multibody System Dynamics **25**(4), 461 – 483 (2011)
24. González, M., González, F., Dopico, D., Luaces, A.: On the effect of linear algebra implementations in real–time multibody system dynamics. Computational Mechanics **41**(4), 607–615 (2008)
25. Kövecses, J.: Dynamics of mechanical systems and the generalized free–body diagram – part I: General formulation. ASME Journal of Applied Mechanics **75**(061012), 1 – 12 (2008)
26. Kövecses, J., Piedbœuf, J.C.: A novel approach for the dynamic analysis and simulation of constrained mechanical systems. In: Proceedings of DETC'03 ASME Design Engineering Technical Conferences, DETC2003/VIB–48318. Chicago, Illinois (2003)
27. Müller, A.: Generic mobility of rigid body mechanisms. Mechanism and Machine Theory **44**(6), 1240 – 1255 (2009)
28. Neto, M.A., Ambrósio, J.: Stabilization methods for the integration of DAE in the presence of redundant constraints. Multibody System Dynamics **10**(1), 81–105 (2003)

29. Rico Martínez, J.M., Ravani, B.: On mobility analysis of linkages using group theory. ASME Journal of Mechanical Design **125**(1), 70–80 (2003)
30. von Schwerin, R.: Multibody System Simulation – Numerical Methods, Algorithms, and Software. Springer (1999)
31. Udwadia, F.E., Kalaba, R.E.: On the foundations of analytical dynamics. International Journal of Non-Linear Mechanics **37**(6), 1079–1090 (2002)
32. Uicker, J.J., Pennock, G.R., Shigley, J.E.: Theory of Machines and Mechanisms, 4th edn. Oxford University Press (2011)
33. Wojtyra, M.: Joint reactions in rigid body mechanisms with dependent constraints. Mechanism and Machine Theory **44**(12), 2265–2278 (2009)
34. Wojtyra, M., Frączek, J.: A comparison of various methods of redundant constraints handling in multibody system dynamics. In: Proceedings of the ASME 2011 International Design Engineering Technical Conferences & Computers and Information in Engineering Conference IDETC/CIE 2011. Washington, DC, USA (2011)
35. Wojtyra, M., Frączek, J.: Joint reactions in overconstrained rigid or flexible body mechanisms. In: Multibody Dynamics 2011, ECCOMAS Thematic Conference. Brussels, Belgium (2011)